Study of mechanical behavior between the rigid and dynamic fixation systems of the spinal column analyzed by the finite element method

S. Zahaf[1, a *], S. Kebdani[a]

[a]Département de génie mécanique, université des sciences et de la technologie d'Oran Mohamed Boudiaf, USTO-MB, BP 1505, EL M'naouer, 31000 Oran Algérie.

Email : kebdani_sd@yahoo.fr

*Corresponding author: samir.zehaf@univ-usto.dz, zahafsamir1983@gmail.com

Keywords: Lumbar spinal stenosis; interspinous; Coflex rivet; Bdyne; Bioflex; Elaspine; Pedicle screw fixation; disc annulus, stress Von Mises; finite element analysis.

Abstract. Orthopedic fixation devices are widely used in treatment of spinal diseases. It is expected that application of dynamic stabilization confers valuable movement possibility besides its main role of load bearing. Comparative investigation between rigid and four dynamic fixation systems may elucidate the efficacy of each design. The goal of the present study is to evaluate the efficacy of five fixation systems mounted on L4-L5 motion segment. In this numerical study, a 3D precious model of L4, L5 and their intervertebral disc has been employed based on CT images. five fixation devices have been also implanted internally to the motion segment. Finite element method was used to evaluate stress distribution in the disc and determine the overall displacement of the segment as a measure of movement possibility. The results show that The Coflex rivet implantation can provide stability in all motions and reduce disc annulus stress at the surgical segment (L4-L5), on the other hand, Maximum stress in the disc has been observed in dynamic systems but within the safe range. The greater movement of the motion segment has been also appeared in dynamic fixations. Existence of the fixation systems reduced the stress on the intervertebral disc which might be exerted in intact cases. Use of the fixation devices can considerably reduce the load on the discs and prepare conditions for healing of the injured ones. Furthermore, dynamic modes of fixation confer possibility of movement to the motion segments in order to facilitate the spinal activities.

Abbreviation :

ALL = anterior longitudinal ligament; PLL = posterior longitudinal ligament; TL = transverse ligament; LF = ligamentum flavum; ISL = interspinous ligament; SSL = supraspinous ligament; CL = capsular ligament; SL = Sacrotuberous Ligament; SPL = Sacroiliac posterior Ligament; IL = Interosseous Ligament); AIB = autogenous iliac bone (AIB); PEEK = polyetheretherketone; ASD = adjacent segment degeneration (ASD); PLIF = posterior lumbar interbody fusion, DIV = disc intervertebral.

1. Introduction

Lumbar spinal stenosis (LSS) is a common disabling disease in the elderly. The reduced disc height narrows the spinal canal and the neural foramina, eventually resulting in nerve compression **[1]**. The symptoms of LSS include bilateral radicular pain and intermittent neurogenic claudication, sensation disturbance and loss of muscle strength in the legs. Many surgeons perform decompression for spinal stenosis and reconstruct the segment with rigid fusion devices. However, rigid fusion may cause increased stress at the adjacent discs,

resulting in degeneration of adjacent segments **[2-4]**. Therefore, flexible non fusion devices such as the interspinous process device were developed with the intention of reducing adjacent segment degeneration.

Spinal disorders (SDs) include a variety of malfunctions in vertebral complex which have been considered as one of the most relevant diseases in the population. SDs can be related to many factors such as occupational conditions, age, weight, etc **[5-8]**, that take considerable costs annually **[7]**. The origin of pain as the main symptom for SDs may be various and elaborative like muscular spasm, weakness or damage **[10]**, damages due to overstretch or overpressure of the existing soft tissue like intervertebral discs (IVD), fascias, tendons and ligaments **[11]**, vertebral damages **[12]**, and spinal cord stimuli **[13]**. In SD cases, the motion segment should be immobilized in order to avoid such movements that deteriorate the case and prevent the healing process **[14].** The first choice is, hence, fusion of the motion segment by rigid instrumentation **[15-19].**

Although the level of stress in the components becomes less in rigid fixation systems, several limitations in back natural motions and discomforts emerge. In a retrospective study, it has been shown that the patient have reported various levels of comfort and satisfaction after the surgery and implantation **[21-22].** Moreover, immobility of one or more segments endangers adjacent segments due to higher share of loading they received followed by revision or re-intervention **[23-29].** These problems have been mastered by using recently-developed systems of fixation, called dynamic stabilization system for the spine **[30-31].** In these designs, the previous rigid rod has been replaced by more flexible alternatives.

For needs of flexibility a spring-shaped connector has been used to provide slight but influencing movement between the vertebrae to perform the kinematic tasks **[32].** Another dynamic fixation system contains polymer spacer between pedicles screws which covers a wire passes through the holes **[32-35].** It has been expected that use of these dynamic systems facilitates the motion of lumbar or thoracic segment underwent fixations.

The dynamic fixation systems, so-called Dynesys, has been employed first by Stoll et al. but then formally introduced by Dubois et al. **[31-36].** Retrospective studies by Cakir et al. showed that Dynesys works slightly better and reduces the operation time and hospital stay, and hence, can be introduced as an effective alternative to fusion in patients **[37].** Kim et al. compared the kinematic behavior of spinal fixation systems, including rigid and dynamic ones by virtual human model at the level of L4-S1. They found that the Dynesys system reveal similar kinematic behaviors to the intact model **[38].**

Cunningham et al. evaluated the safety and efficacy of the Dynesys systems and associated in vitro and in vivo effects in animal models. They used wire and polymer spacer type of Dynesys and concluded that it stabilize spinal motion. Also, 25% rate of screw loosening has been observed after 12 months **[33].** Besides the experimental studies, numerical approaches have been further used to examine the efficacy of the dynamic systems of spinal stabilization.

Shin et al. developed a finite element model of the human lumbar spine to calculate the stiffness of fixation systems implanted on the levels of L2-L5. Their results showed that dynamic stabilization reveals more similar to the intact model rather than fused fixation **[32].** In another study, Zhang et al. conducted a finite element analysis to calculate the bio-mechanical capacity of dynamic fixation systems in type of wire and polymer spacer and stabilization at the level of L4-L5 and indicated that the stiffness of a segment has been increased in dynamic system, thus, it can significantly diminish the intervertebral disc's stress **[34].**

Although the efficacy of the fixation systems have been separately studied, no comparative study exists to shed light on the pros and cons of these systems in a fixed model underwent to the same conditions. Moreover, the measures for the efficiency of the fixation systems vary between stress/strain in IVD and vertebrae, or the displacement of the motion segment. Therefore, the present investigation is aimed at compare the prevalent models of spine fixations including rigid, dynamic systems in a same model and loading conditions using finite element method. The principal aim of the present study was to compare the provision of movement facility for the motion segment against reduction in stress of intervertebral disc.

Fig. 1 shows two vertebrae of the spinal column with an intervertebral disc under the effect of a compound loading (compression P + bending moment P1). The compressive load P creates an internal pressure in the nucleus, this pressure will there after generate the disc degeneration or degenerative disc disease **Fig. 2**, as regards the forward flexion P1, if the load P1 increases, automatically distance between the point of load application and the axis of the spinal column increases, we see that the posterior portion of the annulus fibrosis is tensioned and the other front portion is compressed, that is to say the nucleus pulposus burst back (posterior compression), this compression produced by disc protrusion comes into contact with a nerve root called herniated disc.

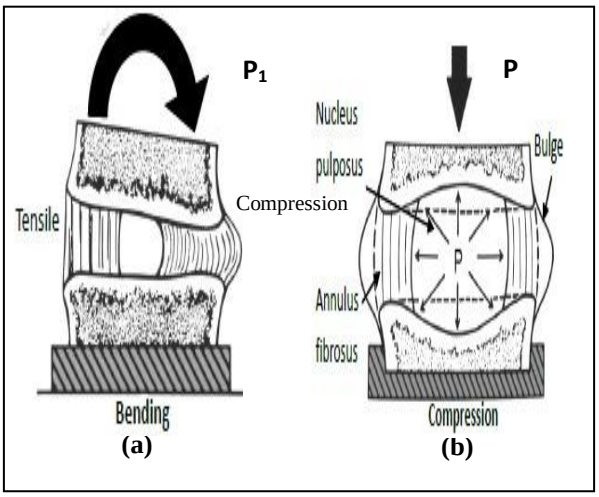


Fig. 1 The intervertebral disc with (a) bending (b) compression **[6].**

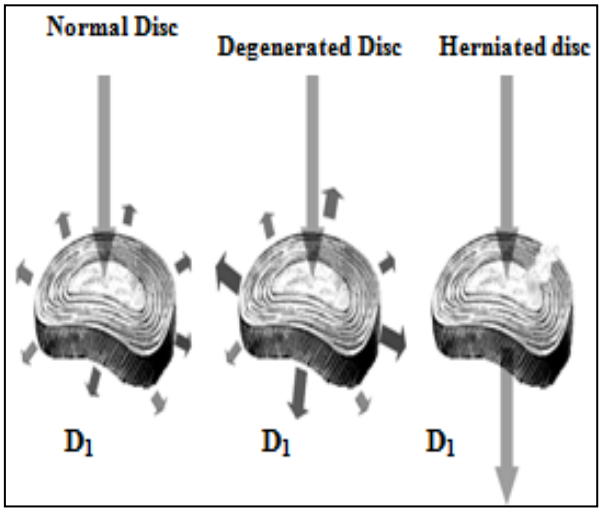


Fig. 2 Load distribution at the disc D1 according to his state **[7]**.

2. Materials and methods

2.1 FE model of intact lumbar spine (intact model)

A validated 3D FE model of the intact L4-L5 segment was used. To create this model, computed tomography scans of the L4-L5 segment of a middle-aged healthy man were obtained at 1-mm intervals. The commercially available FE program, ANSYS 16 (ANSYS Inc., Canonsburg, PA, USA), was used to model the spinal segments. The FE model of the osseoligamentous lumbar segment included the vertebrae, one intervertebral disc, endplates, posterior elements and the following ligaments: supraspinous, interspinous, ligamentum flavum, transverse, posterior longitudinal, anterior longitudinal and capsular. The material properties of the intact L4-L5 segment were assumed to be homogeneous, and a detailed description has been presented in our previous studies **[57–58].** The ligaments were simulated using ten-node link elements with tension resistance only, and the elements were arranged in the anatomic orientation. ten-node solid elements were used for modelling of the cortical bone, cancellous bone, endplate, posterior bony structure and disc.

The disc annulus consisted of fibres embedded in the ground substance. Annular fibres in 6 layers were modelled using ten-node link elements with tension resistance only and placed in an anatomic orientation **[59–61].** The facet joints were treated as nonlinear 3D contact pairs using surface-to-surface contact elements, and the coefficient of friction was set to 0.1 **[57–58].**

The material properties of the INT model are listed in (**Table 1)** and were chosen from previous studies **[39–58].** All seven ligaments were simulated by ten node link elements with resistance tension only, and they were arranged in the anatomical direction given by the text book **[54];** the cross-sectional area of each ligament was obtained from previous studies **[47, 52–54].** An ten-node solid element was used for modeling the annulus ground substance. Cortical bone and cancellous bone were assumed to be homogeneous and isotropic**.** The intervertebral disc consisted of annulus ground substance and nucleus pulposus, which embeds collagen fibers in the ground substance. The nucleus pulposus was modeled as an incompressible fluid with bulk modulus of 1MPa by an ten-node fluid element **[45–53].** The facet joint was treated as a sliding contact problem using surface-to-surface contact elements, and the coefficient of friction was set at 0.1 **[55-56].** The FE model of the intact lumbar spine consisted of 199,689 elements and 32,7621nodes **(Fig. 3).**

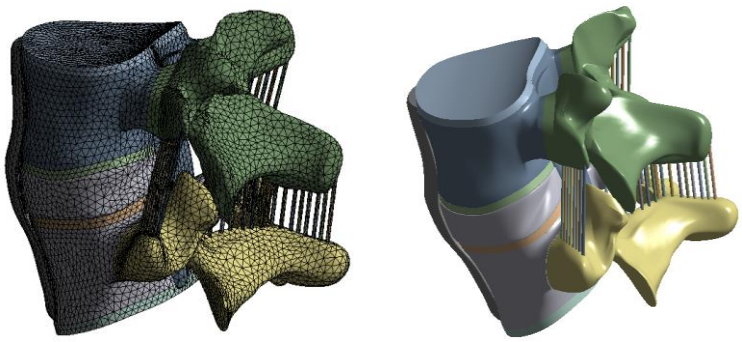


Fig.3 FE model of the L4-L5 Motion Segment with IVD.

2.2 FE model of bilateral B Dyn implant fixation implanted into the L4–L5 segment (B Dyn implant fixation model)

The existing geometrical model of the implant realized with CAO software (Solidworks 2016) was imported. It consists of an assembly of five parts: The piston rod, the cylindrical body, the fixed rod, the ring and the damper block. The contact surfaces between the body and the fixed rod have a threaded area which makes it possible to assemble the implant. In the manufacturing process, after assembly, these two parts are welded together. The geometry of these contact surfaces has therefore been simplified on the geometric model **(Fig. 4)** in order to facilitate the meshing and calculation steps**.** The metal parts (piston rod, cylindrical body and fixed rod) are modeled in titanium TA6V ELi with elastic properties, Young's modulus and Poisson's ratio were assigned to be **112400 MPa** and **0.34**, respectively**.** The deformable parts (ring and damper block) are modeled with an elastic behavior of a silicone, Young's modulus and Poisson's ratio were assigned to be **600 MPa** and **0.49.** The model B Dyn consisted of 228,348elements and 378,676 nodes **(Fig. 4).**

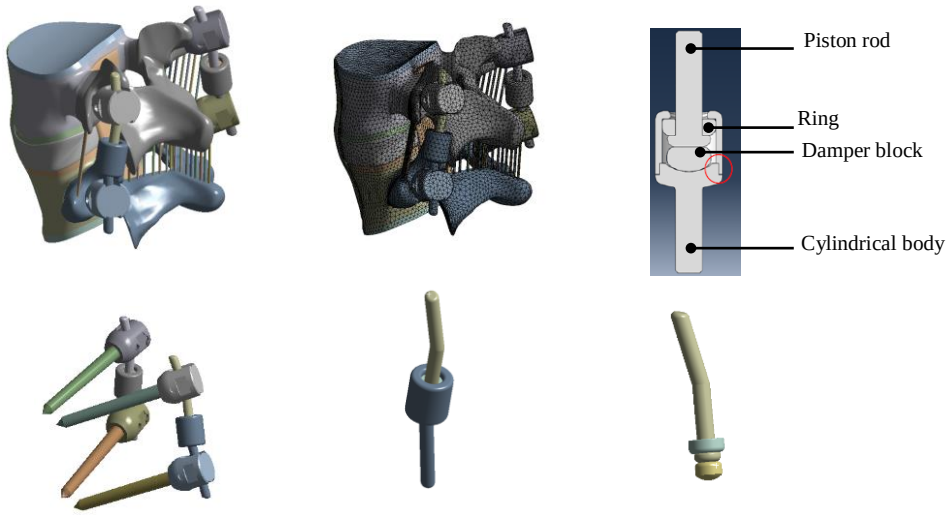


Fig.4 FE model of the L4-L5 Motion Segment with posterior dynamic fixation system **B Dyne.**

2.3 FE model of bilateral ELASPINE implant fixation implanted into the L4–L5 segment (ELASPINE implant fixation model)

The ELASPINE implant consists of six parts: four metal elements made of titanium alloy (Ti6Al4V ISO 5832-3) and two deformable rods made of polymer (silicone). A deformable rod made of polymer (silicone) with a length of 60 mm and a diameter of 7 mm, which is mentioned in **(Fig. 5).** The screw-bone interfaces were assigned to be fully constrained. The material used for the pedicle screws was Ti-6Al-4V. Young's modulus and Poisson's ratio were assigned to be **113000 MPa** and **0.3**, respectively**.** The two deformable parts are modeled with an elastic behavior which contains a Young's modulus and Poisson's ratio were assigned to be 600 MPa and 0.49. The model ELASPINE consisted of 223,950elements and 373,025nodes **(Fig. 5)**. An assembly of two rods and four screws (spinal assembly) is required to stabilize a spinal segment. Each implant is attached to the lumbar vertebrae using titanium pedicle screws **(Fig. 5).**



Fig.5 FE model of the L4-L5 Motion Segment with posterior dynamic fixation system **ELASPINE.**

2.4 FE model of bilateral BIOFLEX implant fixation implanted into the L4–L5 segment (BIOFLEX implant fixation model)

The **BIOFLEX** implant is a helical spring manufactured by the company **BioSpine,** The total length of the rod 70 mm and the spring height 15,7mm, The spring diameter 5mm and the pitch equal 5.5mm. The material used for the BIOFLEX model was Ti-6Al-4V. Young's modulus and Poisson's ratio were assigned to be **113000 MPa** and **0.3**, respectively**.** The **BIOFLEX** model consisted of 228,101elements and 399,240nodes **(Fig. 6).**



Fig.6 FE model of the L4-L5 Motion Segment with posterior dynamic fixation system **BIOFLEX.**

2.5 FE model of Coflexe rivet implanted into the L4–L5 segment (Coflexe rivet model)

The Coflexe rivet model was implanted at the L4–L5 segment. this model was used to simulate instability by cutting the ligamentum flavum, the facet capsules and 50% of the inferior bony facet bilaterally at the L4–L5 segment (Tsai et al. 2006; Kettler et al. 2008). In addition, the supraspinous ligaments and interspinous ligaments had to be resected before insertion.

The Coflex rivet differs from the original Coflex implant by adding two rivets joining the wings and spinous processes **(Fig. 7).** the coefficient of friction for the rest of the contact regions was set to 0.1 **(Fig. 6).**

The rivets were simplified as cylinders and were constrained to both the holes on the wings of the Coflex and the spinous processes in all degrees of freedom (the degrees of freedom of screw nodes are interpolated with the corresponding degrees of freedom of the nodes on the Coflex and spinous processes during the execution of ANSYS program). The material used for the Coflex rivet was a **Ti-6Al-4V** alloy. The Young's modulus and Poisson's ratio, respectively, were assigned to be **113000** MPa and **0.3**, respectively. The model Coflex rivet consisted of 202,615 elements and 332,396 nodes **(Fig. 7).**

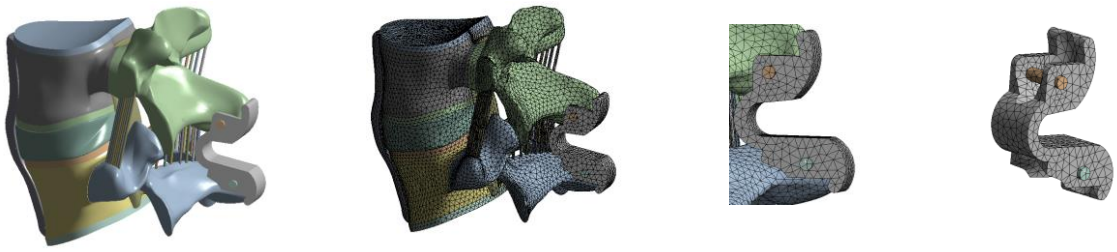


Fig.7 FE model of the L4-L5 Motion Segment with posterior dynamic fixation system **Coflexe rivet.**

2.6 FE model of bilateral pedicle screw fixation implanted into the L4–L5 segment (Pedicle screw fixation model)

The pedicle screw fixation model was implanted at the L4–L5 segment. The difference between the pedicle screw fixation model and the abovementioned implantation models was that the pedicle screw fixation model preserved the supraspinous ligaments and interspinous ligaments **(Fig. 8).** The pedicle screw fixation consisted of two rods (diameter, 5 mm) and four pedicle screws (diameter, 5 mm). The pedicle screws were inserted through the pedicles of the L4 and L5 vertebrae bilaterally. The pedicle screws were simplified as cylinders. The screw-bone interfaces were assigned to be fully constrained. The material used for the pedicle screws was Ti-6Al-4V. Young's modulus and Poisson's ratio were assigned to be **113000 MPa** and **0.3**, respectively**.** The model pedicle screw consisted of 225,769 elements and 394,288 nodes **(Fig. 8).**



Fig. 8 FE model of the L4-L5 Motion Segment with posterior dynamic fixation system **Pedicle screw fixation.**

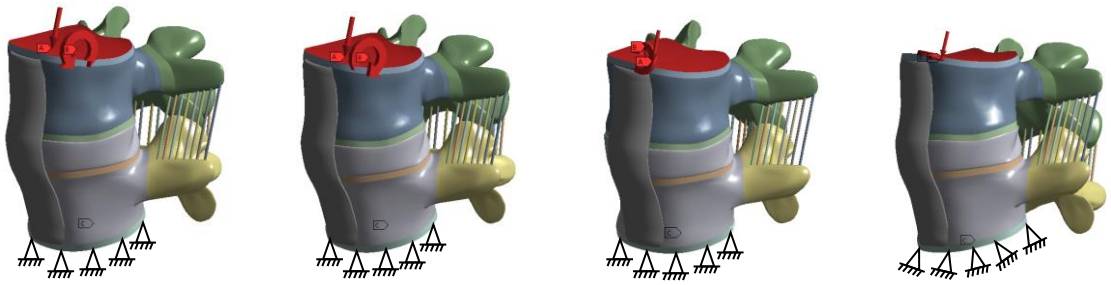
Therefore, the purpose of this work was to study of mechanical behavior between the rigid and dynamic fixation systems of the spinal column by using finite element (FE) analyses on a two-segment spinal model. In addition, Comparative investigation between rigid and 4 dynamic fixation systems may elucidate the efficacy of each design. The goal of the present study is to evaluate the efficacy of four fixation systems mounted on L4-L5 motion segment. Finite element method was used to evaluate stress distribution in the disc and determine the overall displacement of the segment as a measure of movement possibility, the maximal von Mises stress at the disc annulus and the von Mises stress distribution at the surgical disc annulus.

Table 1. Material properties used in the FE model

Material	Young modulus E (MPa)	Poisson coefficient	REFERENCES
Cortical Bone	12000	0.3	[39-45]
Cancellous Bone	100	0.2	[39, 41-42, 44-45]
Posterior Bone	3500	0.25	[39-41, 45-46]
Cartilage Endplates	12000	0.3	[40, 42, 47]
Annulus Ground Substance	4.2	0.45	[39-40, 42, 45, 49-50]
Nucleus Pulposus	1	0.499	[45, 48, 51-53]
Anterior Longitudinal Ligament	7.8 (<12%), 20.0 (>12%)	0.3	[55, 56–58]
Posterior Longitudinal Ligament	10.0 (<11%), 20.0 (>11%)	0.3	[55, 56–58]
Ligamentum Flavum	15.0 (<6.2%), 19.5 (>6.2%)	0.3	[55, 56–58]
Intertransverse Ligament	10.0 (<18%), 58.7 (>18%)	0.3	[55, 56–58]
Inter-Spinous Ligament	10.0 (<14%), 11.6 (>14%)	0.3	[55, 56–58]
Supra-Spinous Ligament	8.0 (<20%), 15.0 (>20%)	0.3	[55, 56–58]
Capsular Ligament	7.5 (<25%), 32.9 (>25%)	0.3	[55, 56–58]

2.7. Boundary and loading conditions

The loading condition was similar to the in vitro study of Yamamoto et al., in which the intact L4-L5 segment was subjected to the maximum possible load without causing spinal injury **[33].** Therefore, all four physiological motions were imposed, each with a moment of 10.6Nm and a compression of 400N on the superior surface of the L4 level. These models constrained all degrees of freedom at the inferior surfaces of the L5 vertebra **(Fig.9).**



(a) **(b)** **(c)** **(d)**

Fig. 9 biomechanical model of the intact L4-L5 segment.
(a): anterior load (flexion), (b): posterior load (extension), (c): lateral load (flexion lateral), (d): axial load (torsion).

3. Results

Two principal functions of the fixation systems were to balance stabilization and dynamization of the motion segment, and also, reduce the overpressure on vulnerable tissues like muscles or IVDs. Therefore, overall displacement of the motion segment and stress of the IVD could be considered as measures for efficacy of the fixation systems.

In flexion, the displacement total of the segment spinal (L4/L5) decreased by 36,81 % in the coflexe rivet model and 29,64 % in the Bioflex model and 22,29 % in the Elaspine model and 21,18 % in the B Dyne model and 2,47 % in the Pedicle screw fixation that the surgical segment **(Fig. 10) .**

On the other hand, the maximum von mises stress of the segment spinal (L4/L5) decreased by 58,80 % in the coflexe rivet model and 41,48 % in the Elaspine model and 39,22% in the B

Dyne model and 16,58 % in the Bioflex model and 3,70 % in the Pedicle screw fixation that the surgical segment.

However, the displacement total of the segment spinal (L4/L5) and maximum Von Mises stress of the intact disc increased by 36,81%, 58,80% in the Coflex rivet model and 2,47%, 3,70% in the pedicle screw fixation model at both the L5–L4 segment.

In extension, the displacement total of the segment spinal (L5/L4) decreased by 20,15% in the coflexe rivet model and 12,80% in the Elaspine model and 8,11% in the B Dyne model and 5% in the pedicle screw and 2,72 in the Bioflexe model at the surgical segment **(Fig. 10)**.

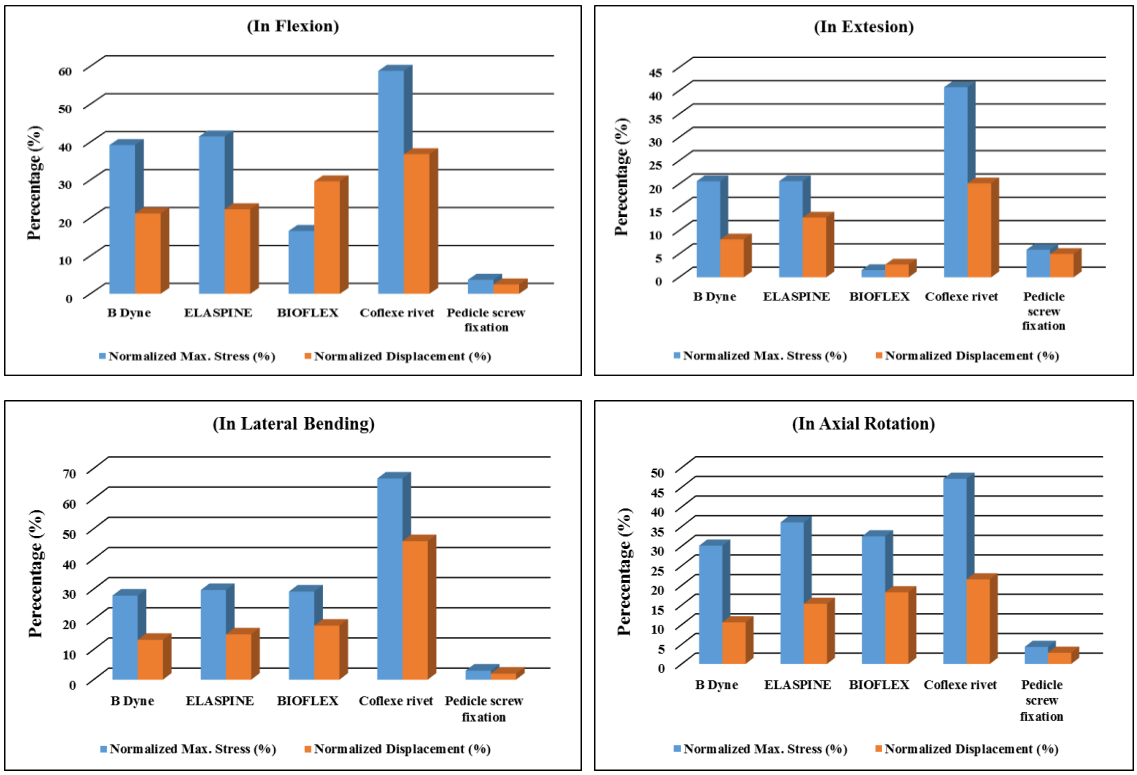


Fig. 10 Maximal von Mises stress of the disc intact model and total displacement of the segment spinal (L4/L5) in flexion, extension, lateral bending and axial rotation for different devices of the rigid posterior fixation system and dynamic.

After implantation, the stress Mises effectively decreased by 40% in the Coflexe rivet mode and 20,61% in the Elaspine model and 20,60% in the B Dyne model and 5,91% in the pedicle screw fixation model and 1,54% in the Bioflexe model when compared with the intact model **.** In addition, the stress Mises are equal in the two models dynamic (B Dyne, Elaspine) but the displacement total of the segment spinal (L5/L4) increased by 12,80% in the Elaspine model and decreased by 8,11% in the B dyne model at both the L5–L4 segment **(Fig. 10)**.

In lateral bending, the displacement total of the segment spinal decreased by 45,89% in the Coflex rivet model, 17,88% in the Bioflexe model and 15,02% in the Elaspine model and 13,18% in the Bdyne model, 1,97% in the pedicle screw fixation model at the surgical segment, when compared with that of the intact model **(Fig. 10)**.

However, the stress Mises in the disc intact decreased by 66,67% in the Coflexe rivet, 29,71% in the Elaspine model, 29,20% in the Bioflex model, 27,86% in the B dyne model, 2,99% in the pedicle screw fixation model at both the L4–L5 segment **(Fig. 10)**.

In axial rotation, the displacement anterior of the segment spinal (L5/L4) decreased by 21,53% in the Coflex rivet model, 18,24% in the Bioflex model and 15,31% in the Elaspine model, 10,57% in the B dyne model, 2,83% pedicle screw fixation model at the surgical segment, when compared with that of the intact model.

However, in the pedicle screw fixation model, the stress Mises decreased by 4,35% at the (L5–L4) segment and increased by 30,12 in the B dyne model, 32,49% in the Bioflex model, 36,05% in the Elaspine model and 47,15% in the Coflexe rivet at the adjacent L4–L5 segment **(Fig. 10)**.

3.1 Maximal Von Mises stress at the disc annulus L4-L5

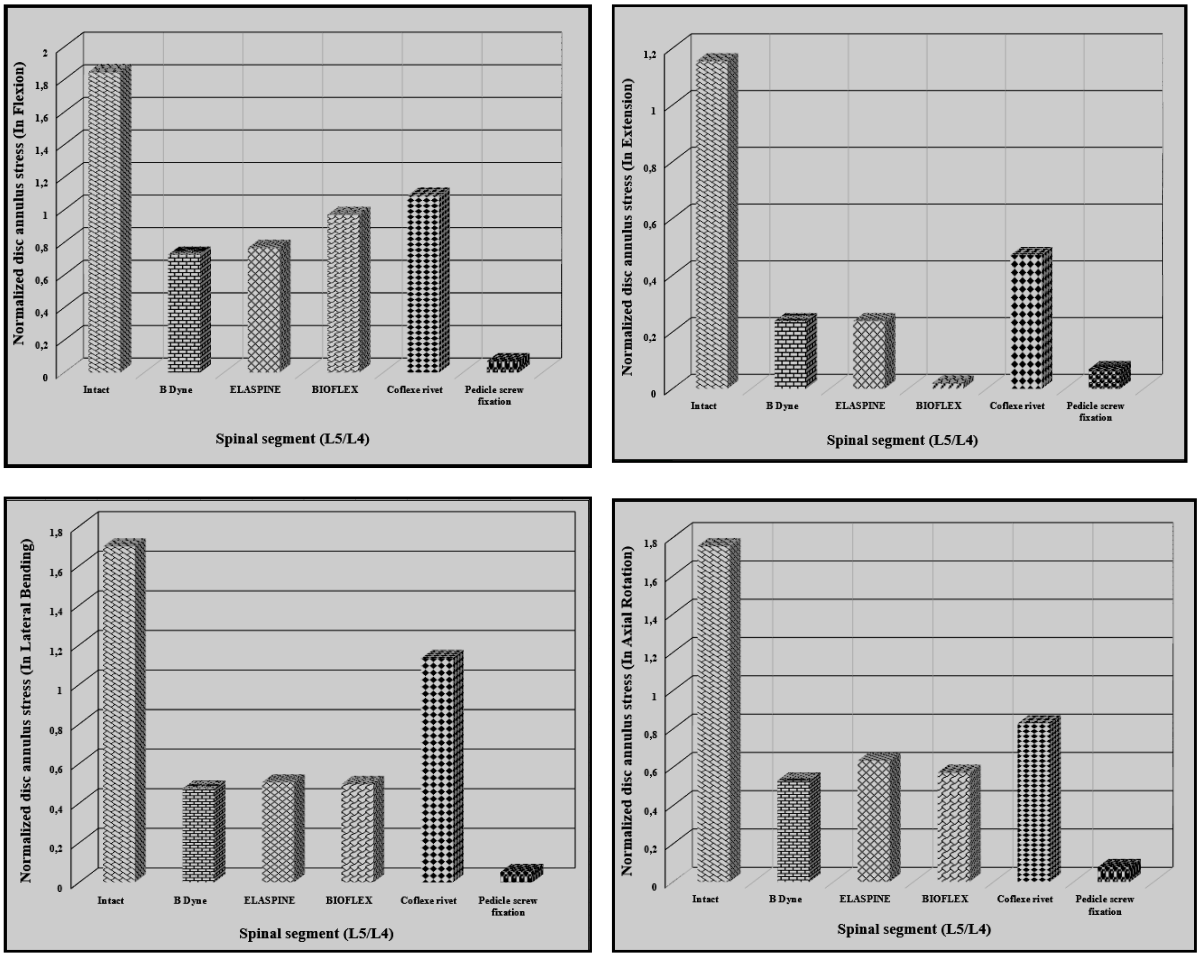


Fig. 11 Maximal von Mises stress of the disc annulus normalised to the intact model in flexion, extension, lateral bending and axial rotation. The B Dyne, Elaspine, Bioflex, pedicle screw fixation models decreased annulus stress at the surgical segment (L4–L5) in flexion and extension. However, the Coflex rivet decreased annulus stress at the surgical segment in both lateral bending and axial rotation.

The highest maximum von mises stress value for the IVD is also appeared in coflexe rivet model, 1,0842 MPa in flexion, 0,47009 MPa in extension, 1,1316 MPa in lateral bending, 0,8263 MPa in axial rotation (**Fig. 11)**.

For the B dyne model, maximum annulus stress at the surgical level (L5/L4) decreased remarkably by 39,22%, 20,60%, 27,86%, and 30,12% in flexion, extension, torsion, and lateral bending, respectively, compared to the INT model (**Fig. 10)**.

For the Elaspine model, the maximum annulus stress at the surgical level decreased remarkably by 41,48%, 20,61%, 29,71%, and 36,05% in flexion, extension, torsion, and lateral bending, respectively, compared to the INT model.

In the model Bioflex, the annulus stress decreased at the surgical L5/L4 level by 16,58%, 1,54%, 29,20%, and 32,49% in flexion, extension, torsion, and lateral bending, respectively **(Fig. 10).**

On the other hand, **(Fig. 10)** clearly shows that the Coflexe rivet model, the maximum annulus stress at the surgical level decreased remarkably by 58,80%, 40,76%, 66,67%, and 47,15% in flexion, extension, torsion, and lateral bending, respectively, compared to the INT model.

We notice in the **(Fig. 10)** that the mixed loading (compression P1 + bending moment (P2)) applied to the upper surface of the lumbar vertebra L4, in the model Pedicle screw fixation the maximum annulus stress at the surgical level decreased remarkably by 3,70%, 5,91%, 2,99%, and 4,35% in flexion, extension, torsion, and lateral bending, respectively, compared to the INT model.

3.2 Stress distribution of the disc annulus (L5–L4)

Fig. 11 presents these contours for 5 models of fixation. Maximum displacement has been revealed in coflexe rivet model by amount of 2,1477 mm in flexion, 0,58024 mm in extension, 2,6188mm in lateral bending, 1,8423mm in axial rotation for the top anterior edge of the vertebral body due to the loading.

Stress concentration and distribution pattern of the disc annulus at the surgical segment changed obviously in these models. In extension, the stress of the five models was concentrated at the posterior–superior regions of the annulus **(Fig. 12).** However, after implantation, the stress concentration of the disc annulus at the posterior disc diminished obviously. Furthermore, in flexion, the stress was concentrated at the anterior of the annulus regions, close to the superior and inferior sides of the endplate **(Fig. 13).**

The Coflex rivet was found to have the most even disc annulus stress distribution in flexion, extension, lateral bending and axial rotation even when compared with the intact model. In lateral bending and axial rotation, the stress was concentrated at the right part of the annulus regions, close to the superior and inferior sides of the endplate in the five models when compared with that of the intact model **(Fig. 14** and **Fig.15).** After implantation, the stress concentration of the disc annulus at the posterior disc was also diminished.

Figure 2 presents these contours for five models of fixation. In flexion and extension, the Maximum displacement has been revealed in Coflexe rivet model by amount of 36,81mm, 20,15mm for the top anterior edge of the vertebral body due to the loading. In lateral bending and axial rotation, the contour of displacement was concentrated in the coflexe rivet model by amount of 45,89mm, 21,53mm for the top anterior edge of the vertebral body due to the loading when compared with that of the intact model **(Fig. 14** and **Fig.15).**

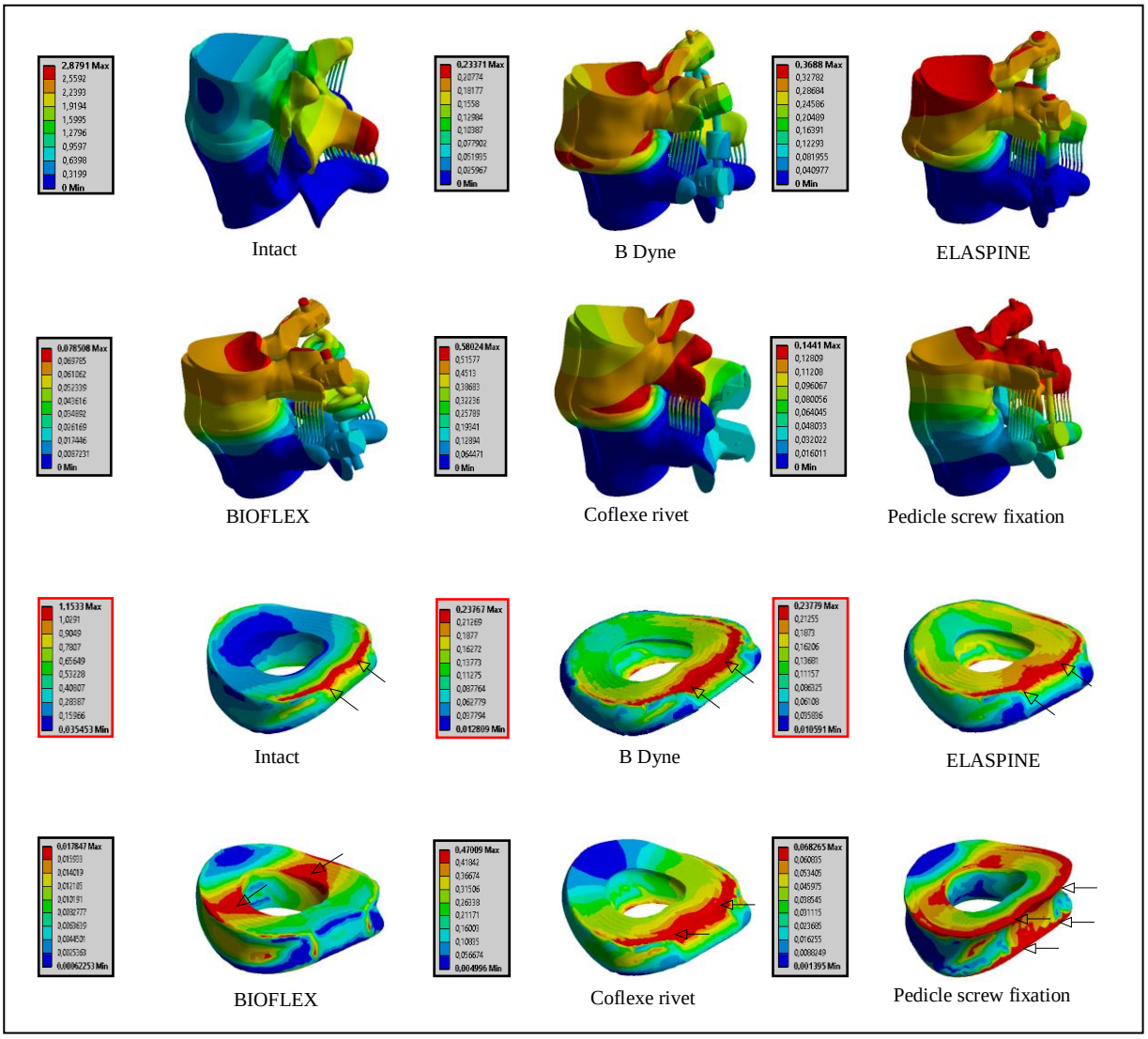


Fig. 12 Displacement total motion segment and Von Mises stress distribution of the surgical segment (L5–L4) disc annulus in extension for various surgical models. The stress of the intact and four models *(B Dyne, ELASPINE, Coflexe rivet, Pedicle screw fixation)* was concentrated at the posterior–superior regions of the annulus, for the BIOFLEX model the stress was concentrated at the left and right regions of the annulus, which were close to the superior and inferior sides of the endplate in the intact model. After implantation, the stress concentration of the disc annulus diminished obviously.

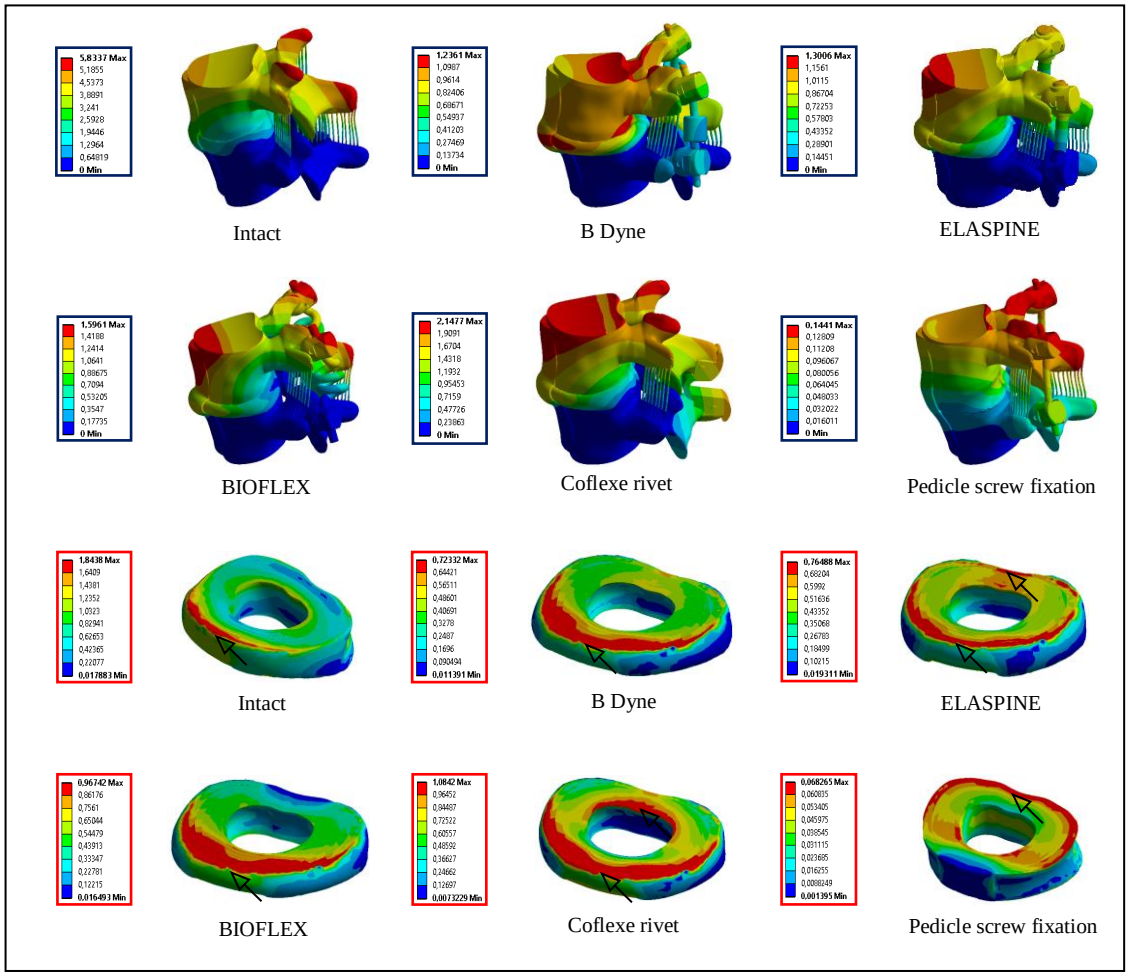


Fig. 13 Stress distribution of the surgical segment (L5–L4) disc annulus in flexion for various surgical models. The stress was concentrated at the superior and inferior regions of the annulus, which were close to the superior and inferior sides of the endplate in the *(B Dyne, Bioflex)* models, for the *Elaspine, Coflexe Rivet, Pedicle Screw Fixation* models the stress was concentrated at the posterior and anterior and regions of the annulus, The Coflex rivet and Bioflex models have the most even disc annulus stress distribution.

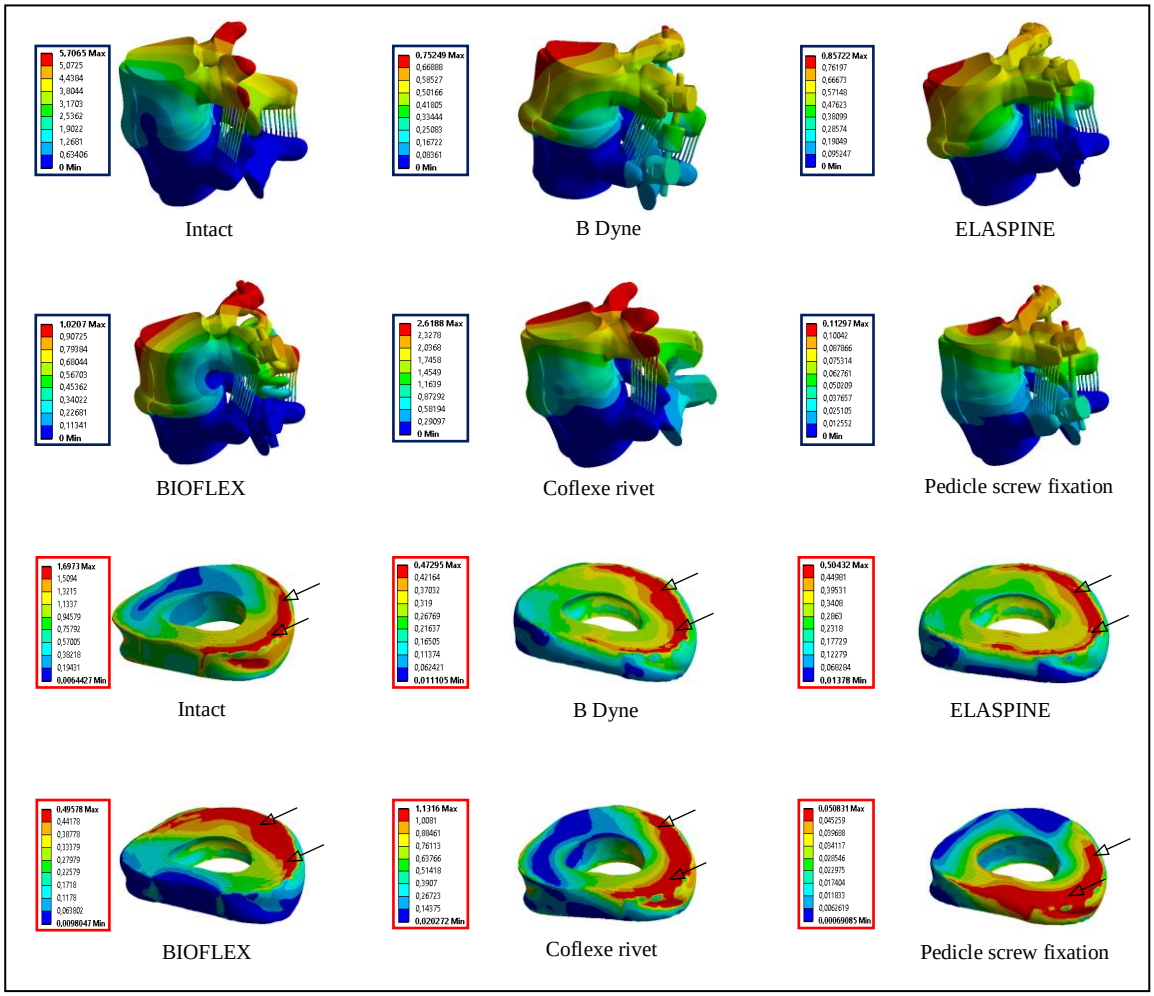


Fig. 14 Stress distribution of the surgical segment (L5–L4) disc annulus in right lateral bending for various surgical models. The stress was concentrated at the right regions of the annulus, which were close to the superior and inferior sides of the endplate in the intact and defect models. The Coflex rivet model have the most even disc annulus stress distribution. After pedicle screw fixation, the stress concentration of the disc annulus diminished obviously.

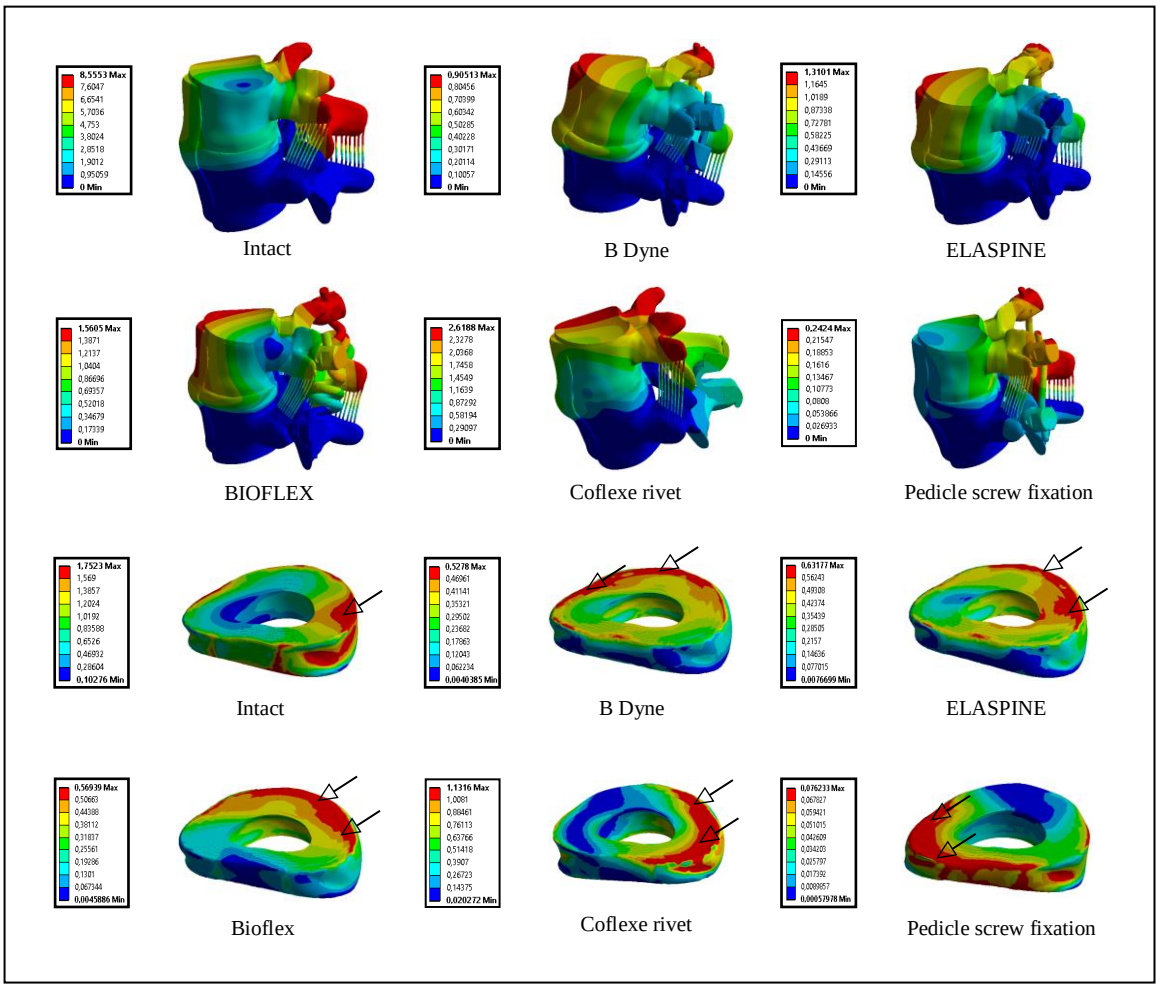


Fig. 15 Stress distribution of the surgical segment (L4–L5) disc annulus in right axial rotation for various surgical models. The stress was concentrated at the right regions of the annulus, which were close to the superior and inferior sides of the endplate in the defect model. After implantation, the stress concentration of the disc annulus diminished obviously.

4. Discussion

A finite element analysis on five models of fixation in order to stabilize L4-L5 motion segment have been performed. Evaluated models were rigid and dynamic fixation systems. Maximum displacement for the whole of the motion segment has been observed in Coflexe rivet model. In flexion, the Bioflex model between 2 vertebrae has permitted the complex to deflect up to 29,64mm for the top anterior edge of the L4 vertebra. In flexion, The Pedicle screw fixation model has revealed relatively less displacement for the motion segment by 2,47% reduction against the coflexe rivet model. Noticeably higher fixation degree of RF system is due to the straight rigid connector rod between the pedicle screws. In such a firm structure a considerable share of the loading energy has been consumed to bend the rigid rod. In RF (pedicle screw fixation) model the overall displacement of the motion segment is associated with the bending deflection of the straight rod.

The Bdyne, Elaspine, Bioflex models, on the other hand, has experienced higher displacement in comparison with pedicle screw fixation model. It may be confusing that how the two models (B Dyne, Elaspine) with an extra component of polymer-spacer (silicone)

received higher movement of displacement; however, noting on the fact that stainless steel rigid connector rod in the pedicle screw fixation model has been replaced by a rod with material of silicone which possesses the Young's modulus approximately half of the RF rod's. Thus, the overall resistance of the fixation system against the external loading (flexion) has been remarkably diminished and maximum displacement in the coflexe rivet became 36,81% greater than in pedicle screw fixation model.

Fundamental diversities in these five models have led to different behavior mecanic of the fixation systems posterior. In the pedicle screw fixation (RF) model rigid rod resists against the loading and the exerted energy has been devoted to bend the rod. In flexion, the two rods of Elaspine model have been strained but the anterior half of the rod of silicone has been compressed and constrained rising of the movement if the motion segment. In Bioflex model, loading energy has been consumed to compress or strained the spring ring but since the compression of the spring directly results in shortening of the ring's ends. in flexion, the overall displacement of the motion segment has been increased up to the maximum value of 1,59mm. It should also be considered that characteristics of the spring provided in the connector rod in Bioflex model is of crucial importance in the results. Diameter if the rod, diameter of the ring, number of the rings and density of the rings per length can influence on the stiffness of such a design.

After implantation, Maximum stress of the IVD has been also occurred in Coflexe rivet model. Provision of the extreme movement for the motion segment resulted in increase of the stress at the anterior regions of the L5-L4 IVD. The maximum stress with these systems of fixation (1,13 MPa) is less than those reported in another numerical works. For instance, in flexion the maximum stress reported for Bioflex model by Zhang et al was roughly 0,96MPa. It has been then concluded that the loading is in medium range of load exertion of the human back based on an in vivo experiments reported that the human in relax standing sustains 0.5 MPa in the IVD for healthy individuals.

In the present study, we also showed that the rivet connecting the metal wings and bony spinous process provides more security than the conventional device. Therefore, the rivet can improve load transmission on the posterior spinal structure to decrease the stress concentration on the disc annulus at the surgical segment in all motions.
However, the Coflex rivet constrained the surgical segment in all motions and it increased displacement at the segments (L5-L4), especially in flexion. Therefore, the Coflex rivet increased annulus stress at both the segment (L5-L4) in flexion and extension.
Several assumptions have been considered in the present numerical analysis. The most important one was to ignore the existence and roles of the muscles acting on vertebral bodies which could also resist against the loading; however, since the goal was to compare the fixation systems, the analysis has neglected them. More, it should be taken into account that loading of analysis was adopted from the Experimental testing. Similar numerical simulations can elucidate the efficacy of such fixation systems in other cases as well.

5. Conclusions

The finite element method (FEM) is a very precise technique used to analyze structural stresses. With its application in engineering, this method can solve many equations to calculate the stresses based on the mechanical properties of the structures being analyzed. FEM has many advantages highlighted by the possibility of including the heterogeneity and irregularity of the contour of the spine in the design of the model and the relative ease with

which the loads can be applied to different directions and sizes for one analysis more complete. The Coflex rivet implantation can provide stability in all motions and can reconstruct the posterior spinal structure for load sharing to reduce disc annulus stress at the surgical segment (L5-L4). However, the Coflex rivet caused a higher displacement and stress at the disc. As a general conclusion, application of the fixation systems can considerably reduce the load on the IVD and prepare conditions for healing of the injured IVD. Furthermore, dynamic modes of fixation, i.e. B Dyne, ELASPINE, BIOFLEX and Coflexe rivet, confer possibility of movement to the motion segments in order to facilitate the spinal activities.

Acknowledgements

The author kindly appreciates Mr. Said Kebdani, and Smail Manssouri for their help in model preparation.

Authors' Contributions

All authors had equal role in design, work, statistical analysis and manuscript writing.

Funding/Support

This paper had been done by personal expenses.

[1] Arbit E, Pannullo S, Lumbar stenosis: a clinical review, Clin Orthop. 384 (2001) 137–143.

[2] Kuslich SD, Danielson G, Dowdle JD, Sherman J, Fredrickson B, Yuan H, Griffith SL, Four-year follow-up results of lumbar spine arthrodesis using the Bagby and Kuslich lumbar fusion cage, Spine. 25(20) (2000) 2656–2662.

[3] Lai PL, Chen LH, Niu CC, Fu TS, Chen WJ. Relation between laminectomy and development of adjacent segment instability after lumbar fusion with pedicle fixation, Spine. 29(22) (2004) 2527–2532.

[4] Zucherman JF, Hsu KY, Hartjen CA, Mehalic TF, Implicito DA, Martin MJ, Johnson DR, II, Skidmore GA, Vessa PP, Dwyer JW, Puccio S, Cauthen JC, Ozuna RM, A prospective randomized multi-center study for the treatment of lumbar spinal stenosis with the X STOP interspinous implant: 1-year results, Eur Spine J. 13(1) (2004) 22–31.

[5] Walker BF. The prevalence of low back pain: a systematic review of the literature from 1966 to 1998. J Spinal Disord.13(3) (2000) 205–17.

[6] Mazloum A, Nozad H, Kumashiro M. Occupational low back pain among workers in some small-sized factories in Ardabil, Iran. Ind Health. 2006;**44**(1):135–9.

[7] Marras WS, Lavender SA, Leurgans SE, Fathallah FA, Ferguson SA, Allread WG, et al. Biomechanical risk factors for occupationally related low back disorders. Ergonomics. 1995;**38**(2):377–410.

[8] Jeong GK, Bendo JA. Spinal disorders in the elderly. Clin Orthop Relat Res. 2004; (425):110–25.

[9] Marras WS. Occupational low back disorder causation and control. Ergonomics. 2000;**43**(7):880–902.

[10] Hides JA, Stokes MJ, Saide M, Jull GA, Cooper DH. Evidence of lumbar multifidus muscle wasting ipsilateral to symptoms in patients with acute/subacute low back pain. Spine (Phila Pa 1976). 1994;**19**(2):165–72.

[11] Sullivan MJL, Stanish W, Waite H, Sullivan M, Tripp DA. Catastrophizing, pain, and disability in patients with soft-tissue injuries. Pain. 1998;**77**(3):253–60.

[12] Nevitt MC, Ettinger B, Black DM, Stone K, Jamal SA, Ensrud K, et al. The association of radiographically detected vertebral fractures with back pain and function: a prospective study. Ann Intern Med. 1998;**128**(10):793–800.

[13] Turner JA, Loeser JD, Bell KG. Spinal cord stimulation for chronic low back pain: a systematic literature synthesis. Neurosurgery. 1995;**37**(6):1088–95.

[14] Putzier M, Schneider SV, Funk J, Perka C. [Application of a dynamic pedicle screw system (DYNESYS) for lumbar segmental degenerations - comparison of clinical and radiological results for different indications]. Z Orthop Ihre Grenzgeb. 2004;**142**(2):166–73.

[15] Harrington PR, Dickson JH. Spinal Instrumentation in the Treatment of Severe Progressive Spondylolisthesis. Clin Orthop Relat Res. 1976;(117):157–63.

[16] Magerl FP. Stabilization of the Lower Thoracic and Lumbar Spine with External Skeletal Fixation. Clin Orthop Relat Res. 1984;(189):125–41.

[17] Dick W, Kluger P, Magerl F, Woersdorfer O, Zach G. A new device for internal fixation of thoracolumbar and lumbar spine fractures: the 'fixateur interne'. Paraplegia. 1985;**23**(4):225–32.

[18] Roy-Camille R, Saillant G, Berteaux D, Marie-Anne S, Mamoudy P. [Vertebral osteosynthesis using metal plates. Its different uses (author's transl)]. Chirurgie. 1979;**105**(7):597–603.

[19] Steffee AD, Biscup RS, Sitkowskj DJ. Segmental Spine Plates with Pedicle Screw Fixation A New Internal Fixation Device for Disorders of the Lumbar and Thoracolumbar Spine. Clin Orthop Relat Res. 1986;(203):45–53.

[20] Turner JA, Ersek M, Herron L, Haselkorn J, Kent D, Ciol MA, et al. Patient outcomes after lumbar spinal fusions. JAMA. 1992;268(7):907–11.

[21] Buttermann GR, Garvey TA, Hunt AF, Transfeldt EE, Bradford DS, Boachie-Adjei O, et al. Lumbar fusion results related to diagnosis. *Spine (Phila Pa 1976)*. 1998;**23**(1):116–27.

[22] Thomsen K, Christensen FB, Eiskjaer SP, Hansen ES, Fruensgaard S, Bunger CE. 1997 Volvo Award winner in clinical studies. The effect of pedicle screw instrumentation on functional outcome and fusion rates in posterolateral lumbar spinal fusion: a prospective, randomized clinical study. Spine (Phila Pa 1976). 1997;22(24):2813–22.

[23] Aota Y, Kumano K, Hirabayashi S. Postfusion instability at the adjacent segments after rigid pedicle screw fixation for degenerative lumbar spinal disorders. *J Spinal Disord Tech*. 1995;**8**(6):464–73.

[24] Rahm MD, Hall BB. Adjacent-Segment Degeneration After Lumbar Fusion with Instrumentation. J Spinal Disord. 1996;9(5):392–400.

[25] Schlegel JD, Smith JA, Schleusener RL. Lumbar motion segment pathology adjacent to thoracolumbar, lumbar, and lumbosacral fusions. *Spine (Phila Pa 1976)*. 1996;**21**(8):970–81.

[26] Schulitz KP, Wiesner L, Wittenberg RH, Hille E. [The mobile segment above fusion]. *Z Orthop Ihre Grenzgeb*. 1996;**134**(2):171–6.

[27] Lehmann TR, Spratt KF, Tozzi JE, Weinstein JN, Reinarz SJ, el-Khoury GY, et al. Long-term follow-up of lower lumbar fusion patients. *Spine (Phila Pa 1976)*. 1987;**12**(2):97–104.

[28] Whitecloud T, Davis JM, Olive PM. Operative Treatment of the Degenerated Segment Adjacent to a Lumbar Fusion. Spine. 1994;19(5):531–6.

[29] Bastian L, Lange U, Knop C, Tusch G, Blauth M. Evaluation of the mobility of adjacent segments after posterior thoracolumbar fixation: a biomechanical study. *Europ Spine J*. 2001;**10**(4):295–300.

[30] Schwarzenbach O, Berlemann U, Stoll TM, Dubois G. Posterior dynamic stabilization systems: DYNESYS. *Orthop Clin North Am*. 2005;**36**(3):363–72.

[31] Stoll TM, Dubois G, Schwarzenbach O. The dynamic neutralization system for the spine: a multi-center study of a novel non-fusion system. *Eur Spine J*. 2002;**11 Suppl 2**:S170–8.

[32] Shin DS, Lee K, Kim D. Biomechanical study of lumbar spine with dynamic stabilization device using finite element method. *Com-Aid Desig*. 2007;**39**(7):559–67.

[33] Cunningham BW, Dawson JM, Hu N, Kim SW, McAfee PC, Griffith SL. Preclinical evaluation of the Dynesys posterior spinal stabilization system: a nonhuman primate model. *Spine J*. 2010;**10**(9):775–83.

[34] Zhang QH, Zhou YL, Petit D, Teo EC. Evaluation of load transfer characteristics of a dynamic stabilization device on disc loading under compression. *Med Eng Phys*. 2009;**31**(5):533–8.

[35] Schmoelz W, Huber JF, Nydegger T, Dipl I, Claes L, Wilke HJ. Dynamic stabilization of the lumbar spine and its effects on adjacent segments: an in vitro experiment. *J Spinal Disord Tech*. 2003;**16**(4):418–23.

[36] Dubois G, De Germay B, Schaerer NS. Dynamic neutralization. In: Szpalski M, Gunzburg R, Pope MH; editors. *A new concept for restablization of the spine*. Philadelphia: Lippincott Williams & Wilkins; 1999.

[37] Cakir B, Ulmar B, Koepp H. [Posterior dynamic stabilization as an alternative for dorso-ventral fusion in spinal stenosis with degenerative instability]. *Z Orthop Ihre Grenzgeb*. 2002;**141**(4):418–24.

[38] Kim SM, Yang I, Lee SY, Cho SY. Dynamic simulation of universal spacer in Dynesys dynamic

stabilization system for human vertebra. *Trans Nonfer Metal Soci China.* 2009;**19**:s238–42.

[39] Natarajan RN and Andersson GBJ. Modeling the annular incision in a herniated lumbar intervertebral disc to study its effect on disc stability. Comput Struct 1997; 64: 1291-7.

[40] Pitzen T, Geisler FH, Matthis D, Storz HM, Pedersen K and Steudel WI. The influence of cancellous bone density on load sharing in human lumbar spine: a comparison between an intact and a surgically altered motion segment. Eur Spine J 2001; 10:23-9.

[41] Polikeit, A: Finite element analysis of the lumbar spine: Clinical application. Inaugural dissertation, University of Bern, 2002.

[42] Denozi´ere G. Numerical modeling of a ligamentous lumber motion segment, M.S. thesis, Department of Mechanical Engineering, Georgia Institute of Technology, Georgia, USA, 2004.

[43] Baroud, G., Nemes, J., Heini, P., and Steffen, T.: Load shift of the intervertebral disc after a vertebroplasty: a finite element study. Eur Spine J 2003; 12: 421-6.

[44] Gwanseob Shin: Viscoelastic responses of the lumbar spine during prolonged stooping. Ph.D. dissertation, NCSU, USA, 2005.

[45] Sairyo K, Goel VK, Masuda A, Vishnubhotla S, Faizan A, Biyani A, Ebraheim N, Yonekura D, Murakami RI and Terai T. Three-dimensional finite element analysis of the pediatric lumbar spine. Eur Spine J 2006; 15:923-9.

[46] Rohlmann A, Burra NK, Zander T, Bergmann G. Comparison of the effects of bilateral posterior dynamic and rigid fixation devices on the loads in the lumbar spine. Eur Spine J 2007; 16:1223-31.

[47] Goel VK, Monroe BT, Gilbertson LG, Brinckmann P. Interlaminar shear stresses and laminae separation in a disc. Finite element analysis of the L3–L4 motion segment subjected to axial compressive loads. Spine 1995;20:689–98.

[48] Smit T, Odgaard A, Schneider E.Structure and function of vertebral trabecular bone. Spine 1997; 22:2823-33.

[49] Sharma M, Langrana NA, Rodriguez J. Role of ligaments and facets in lumbar spinal stability. Spine 1995; 20: 887-900.

[50] Lee KK, Teo EC. Effects of laminectomy and facetectomy on the stability of the lumbar motion segment. Med Eng Phys 2004; 26:183-92.

[51] Rohlmann A, Zander T, Schmidt H, Wilke HJ, Bergmann G. Analysis of the influence of disc degeneration on the mechanical behaviour of a lumbar motion segment using the finite element method. J Biomech 2006; 39:2484-90.

[52] Shirazi-Adl A, Ahmed AM, Shrivastava SC. Mechanical response of a lumbar motion segment in axial torque alone and combined with compression. Spine 1986;11:914–27.

[53] White 3rd AA, Panjabi MM. Clinical biomechanics of the spine. 2nd ed. Philadelphia/Toronto: J.B. Lippincott Company; 1990.

[54] Lee KK, Teo EC, Fuss FK,VanneuvilleV, Qiu TX, NgHW, et al. Finiteelement analysis for lumbar interbody fusion under axial loading. IEEE Trans Biomed Eng 2004;51:393–400.

[55] Polikeit A, Ferguson SJ, Nolte LP, Orr TE. Factors influencing stresses in the lumbar spine after the insertion of intervertebral cages: finite element analysis. Eur Spine J 2003;12:413–20.

[56] Chen CS, Cheng CK, Liu CL, Lo WH. Stress analysis of the disc adjacent fusion in lumbar spine. Med Eng Phys 2001;23:483–91.

[57] Chen SH, Zhong ZC, Chen CS, Chen WJ, Hung C. 2009. Biomechanical comparison between lumbar disc arthroplasty and fusion. Med Eng Phys. 31(2):244–253.

[58] Zhong ZC, Chen SH, Hung CH. 2009. Load- and displacementcontrolled finite element analyses on fusion and non-fusion spinal implants. Proc Inst Mech Eng H. 223(2):143–157.

[59] Eberlein R, Holzapfel GA, Schulze-Bauer CAJ. 2001. An anisotropic constitutive model for annulus tissue, and enhanced finite element analysis of intact lumbar disc bodies. Comput Methods Biomech Biomed Engin. 4(3): 209–230.

[60] Vena P, Franzoso G, Gastaldi D, Contro R, Dallolio V. 2005. A finite element model of the L4–L5 spinal motion segment: biomechanical compatibility of an interspinous device. Comput Methods Biomech Biomed Engin. 8(1):7–16.

[61] Schmidt H, Heuer F, Simon U, Kettler A, Rohlmann A, Claes L, Wilke HJ. 2006. Application of a new calibration method for a 3D finite element model of a human lumbar annulus fibrosus. Clin Biomech. 21(4):337–344.